ELSEVIER

Self-assembly monolayer of anatase titanium oxide from solution process on indium tin oxide glass substrate for polymer photovoltaic cells

Chun-Hao Huang [a,b], Chia-Hua Huang [c], Thien-Phap Nguyen [a,*], Chain-Shu Hsu [b]

[a] *Laboratoire de Physique des Matériaux et Nanostructues, Institut des Matériaux Jean Rouxel, 2 rue de la Houssinière, BP32229, 44322 Nantes, France*
[b] *Department of Applied Chemistry, National Chiao Tung University, Hsinchu 30010, Taiwan, R.O.C.*
[c] *Department of Electrical Engineering, National Dong Hwa University, Hualien 97401, Taiwan, R.O.C.*

Available online 25 January 2007

Abstract

Titanium dioxide (TiO_2) thin films were deposited on indium tin oxide (ITO) coated glass substrates by a liquid phase deposition method using two different precursor concentrations of 0.01 M and 0.005 M $[NH_4]_2TiF_6$. Characterizations of the deposited TiO_2 films were performed by using different spectroscopic techniques including X-ray photoelectron spectroscopy, Raman spectroscopy and X-ray diffraction. From scanning electron microscopy observation, the surface of the TiO_2 films show a ricelike morphology. We have fabricated polymer-based photovoltaic cells (PCs) using the studied TiO_2 films and compared their performances to those using bare ITO-coated glass substrates. The structure of the PCs is glass/ITO/TiO_2/PCBM:P3HT/Au where PCBM:P3HT is poly(3-hexylthiophene) and [6,6]-phenyl-C61-butyric acid methyl ester. The power conversion efficiency of these devices is determined to be 0.85%, which is higher than that of similar devices without TiO_2 films (0.13%).
© 2007 Elsevier B.V. All rights reserved.

Keywords: Titanium dioxide; Liquid phase deposition; Polymer photovoltaic cells

1. Introduction

Thanks to its unique chemical, electronic and optical properties, titanium dioxide (TiO_2) thin films are interesting for various applications including microelectronics [1], solar energy conversion [2], photocatalysts [3], and organic light emitting diodes [4]. Many preparation methods of TiO_2 thin films have been successfully developed: by dry process such as chemical vapor deposition, or by wet process such as the sol–gel method. However, these processes using vacuum conditions require expensive equipments and several problems for depositing large area substrates have been retrieved and still to be solved. In recent years, a novel wet method, named liquid phase deposition or LPD [5–7] has been developed, which allows deposition of TiO_2 films on immersed substrates such as silicon, glass and polymer in an aqueous solution containing a halogenate titanium compound. The advantages of this process are the possibility to deposit on TiO_2 films on large area substrates, at low temperature and without expensive equipments.

Besides, TiO_2 it has been reported as an electron acceptor and transport material for photovoltaic (PV) dye-sentitized cells [8,9], hybrid polymer/TiO_2 cells [10–12], and hole transport materials/ dye/TiO_2 cells [13,14]. To our knowledge, the LPD method for the deposition of TiO_2 layer has not been used in PV device until now. In this paper, we have deposited the TiO_2 thin films on ITO-coated glass substrate at 50 °C using ammonium hexafluoroti-tanate ($[NH_4]_2TiF_6$) and bromic acid (H_3BO_3) aqueous solution. We defined the optimum preparation conditions for obtaining thin films with good morphology and we then used these substrates for fabrication of organic devices. When a TiO_2 thin film is inserted between the anode and the polymer film of polymer-based photovoltaic cells, not only there will be no direct contact between the these layers, that would prevent diffusion of metallic atoms, but an enhancement of the device power conversion efficiency is also expected due to the improvement of the charge injection by the presence of the oxide layer.

2. Experimental

TiO_2 thin films was prepared by hydrolysis of $[NH_4]_2TiF_6$ and H_3BO_3. Aqueous solutions of $[NH_4]_2TiF_6$ and H_3BO_3 were separately dissolved in deionized water at 50 °C for 1 h. H_3BO_3

---

solution was then mixed with [NH₄]TiF₆ solution and an appropriate amount of HCl solution was added to the solution to control the pH. For the deposition process, a pre-cleaned indium-tin-oxide (ITO) glass was immersed in the solution containing either 0.01M [NH₄]TiF₆ and 0.03M H₃BO₃ (solution 01) or 0.005 M [NH₄]TiF₆ and 0.015M H₃BO₃ (solution 02). Both solutions were kept in similar conditions of pH (2.5) and temperature (50 °C). After 8 h, the substrates were taken out and rinsed with distilled water in ultrasonic bath for 30 min to remove unbound TiO_2 particles on the ITO surface. They were then dried in air and at room temperature.

X-ray photoelectron spectroscopy (XPS) measurements were carried on a Leybold LHS-12 spectrometer (Université de Nantes-CNRS), using a magnesium cathode ($h\nu = 1253.6$ eV), operating at 12 kV and 10 mA. The energy pass was set at 25 eV for all experiments. The pressure of the chamber was kept in the 10^{-9} mbar range during analysis. Raman spectra were recorded on a RFS 100 Bruker spectrometer and X-ray diffraction (XRD) experiments were carried out using a Siemens D5000 system, the samples being kept at room temperature and in air.

The polymer used as an active layer in PV devices was a blend of poly(3-hexylthiophene) and [6,6]-phenyl-C61-butyric acid methyl ester (P3HT:PCBM) mixed in 1:1 weight ratio and dissolved in chlorobenzene solution (20% in wt/v). The PV cells were prepared according to the following procedure. The ITO/TiO_2 substrates were cleaned with isopropanol in a ultrasonic bath and dried in a nitrogen flow. In a glove box, a polymer thin film was deposited by spin-coating the solution onto ITO/TiO_2 substrates at a rate of 800 rpm. The sample was then heated at 140 °C for 20 min in the glove box. A gold (Au) cathode was deposited under high vacuum conditions ($<10^{-6}$ mbar) to form ITO/TiO_2/ P3HT:PCBM/Au structure. Four PV cells of active area of 10 mm² each were fabricated on a same substrate. The thicknesses of the films were 80−100 nm for TiO_2 thin films, 100–150 nm for the polymer layer, and 100 nm for the gold anode film.

The current–voltage characteristics of devices were measured with a class A xenon-arc solar simulator under the standard conditions (AM1.5 spectrum, 1000 W/m²). The solar simulator was calibrated with a reference cell calibrated by National Renewable Energy Laboratory.

3. Results and discussion

3.1. Characterization of TiO_2 thin films

For practical applications in organic devices, it is important to obtain a thin oxide film with a smooth morphology. For optimizing the film deposition, several process parameters such as nature of the substrate, solution pH, temperature, reaction time and concentration of precursor have been examined. To observe the surface thin film, the obtained sample was analysed by scanning electron microscopy (SEM). On glass substrates, whatever the synthesis parameters, a uniform surface of the oxide film could not be obtained. The oxide particles tend to aggregate, forming isolated islands with flowerlike morphology. When a high concentration was used, a continuous film was formed but its thickness is important and cracks were observed. On ITO glass

substrates, by adjusting the synthesis parameters, which are given in the experimental part, uniform thin films of TiO_2 could be obtained. Fig. 1 shows two different morphologies of the oxide films obtained by using a precursor (NH₄)₂TiF₆ solution at different concentrations 0.005 M and 0.01 M The TiO_2 particles exhibit a spherical ricelike morphology for two different precursor concentrations. Their size depends also on the concentration of [NH₄]TiF₆, approximately 100 nm for 0.01 M and 80 nm for 0.005 M. The particle density and the thickness of the film are also function of the precursor concentration. In Fig. 1c, the cross section of a film prepared with a 0.01 M solution is shown. The thickness
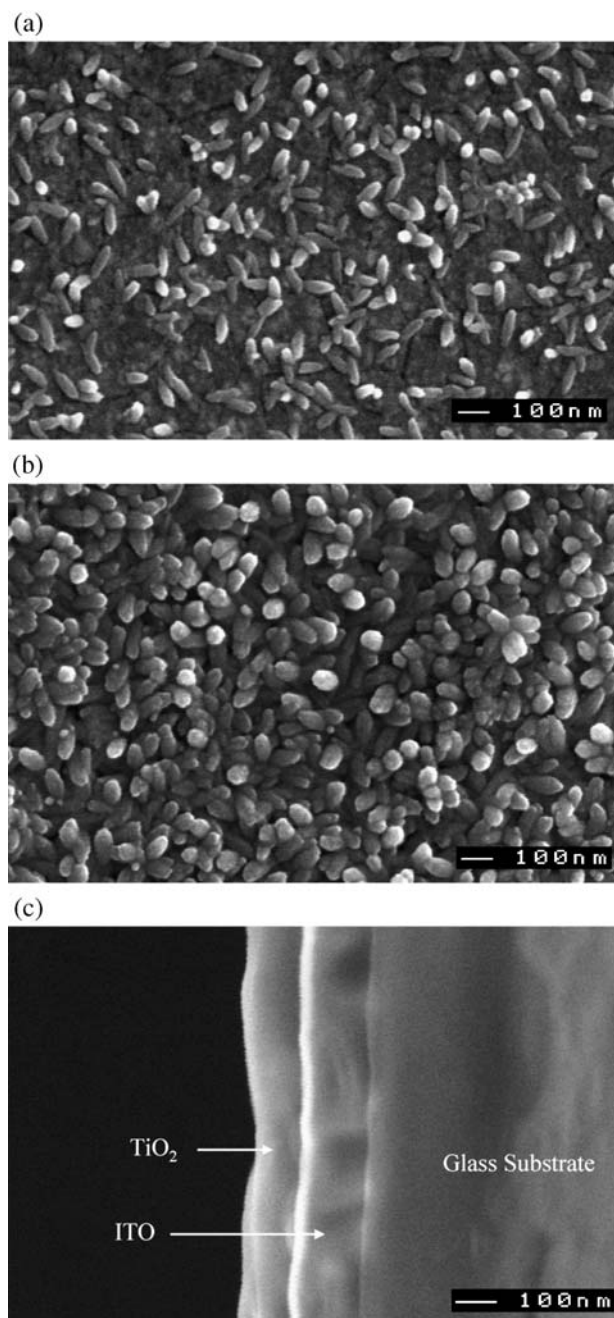

Fig. 1. SEM images of a TiO_2 layer: a) prepared with 0.005 M [NH₄]TiF₆ (top view); b) prepared with 0.01 M [NH₄]TiF₆ (top view); c) prepared with 0.01 M [NH₄]TiF₆ (cross section view).
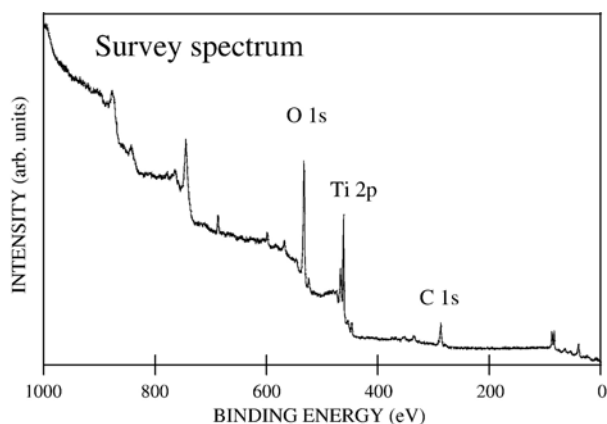
Fig. 2. XPS survey spectra of TiO₂ thin films deposited on ITO substrate.

of the film is approximately 100 nm, while using lower concentration, thinner films could be obtained. To our knowledge, those are the thinnest TiO₂ films obtained by LPD process.

The uniform oxide films obtained by the used technique are expected to form a good mechanical and electrical contact with the deposited polymer layer, and the high quality contact would favor the charge injection into the active layer.

The oxide films were further analysed by several spectroscopy techniques. Fig. 2 shows the XPS survey spectra of TiO₂ thin films deposited on ITO glass substrate. The titanium peaks were located at 465.0 eV (Ti $p_{3/2}$) and 458.6 eV (Ti $p_{5/2}$), which correspond to TiO₂. The oxygen line O 1s is peaked at 530.6 eV corresponding to (Ti^{4+}-O) bonding, in agreement with literature data [15]. We observe that a peak is set at 684.8 eV, which corresponds to F 1s line and is attributed to fluorine residual products. The XRD pattern for TiO₂ film deposited on ITO-coated glass is presented in Fig. 3. The X-rays peaks corresponding to (101), (004), (200) and (211) planes could be retrieved from the diagram, the other peaks being attributed to the ITO-coated glass. The most pronounced peak corresponds to (101) planes as already observed in films deposited on different substrates such as silicon or quartz [16,17]. We have further analysed the TiO₂ films by Raman spectroscopy (not shown). Several vibrational bands centered at 162, 419, 505
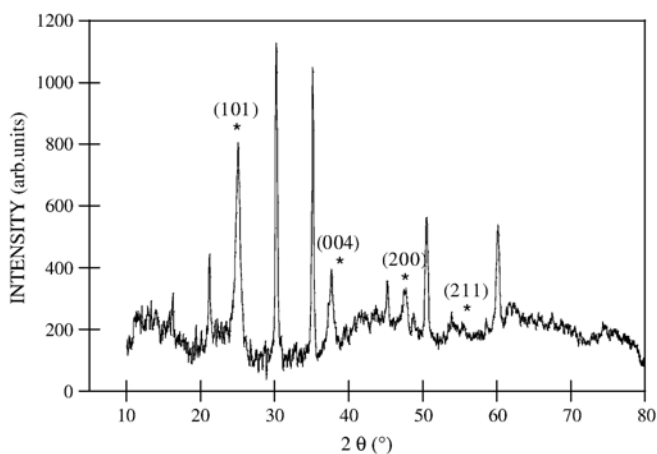

Fig. 3. XRD patterns of prepared TiO₂ thin films on ITO substrate.
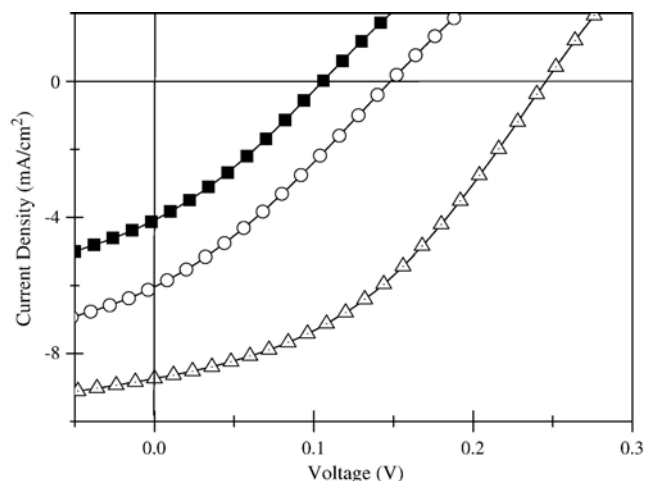

Fig. 4. Current density–voltage characteristics of photovoltaic devices A (ν), B (Υ) and C (Δ) (see text).

and 618 cm^{-1}, are retrieved which can be related to the anatase phase of TiO₂ (Eg, A1g, B1g, and Eg).

In summary, the technique we used here provides smooth surface and uniform TiO₂ thin films on ITO substrates, of thickness of about ∼ 100 nm. These films are sufficiently thin to be incorporated to organic device structure in order to improve their performance.

3.2. Characterization of polymer-based photovoltaic devices

In order to check the influence of the TiO₂ layer on the performance of solar cells, we have prepared different structures using PCBM:P3HT as an active layer. The devices studied were the followings: glass/ITO/PCBM:P3HT/Au (device A), glass/ITO/TiO₂ (0.005 M)/PCBM:P3HT/Au (device B), and glass/ITO/TiO₂ (0.01 M)/PCBM:P3HT/Au (device C). Fig. 4 shows the current–voltage characteristics of these devices under illumination. It is clear that their behaviors are different and their photovoltaic performance was summarized in Table 1. We note that the devices B and C have better efficiencies than device A (0.27 and 0.85% compared to 0.13%). On the other hand, the fill factors are similar for devices A and B (30) but higher for device C (40). It should be borne in mind that the devices studied here are bulk heterojunction ones [18] using a blend of P3HT and PCBM as an active layer. The improvement of the performance can be explained as follows. In dye-sensitized solar cells, titanium dioxide layer, as a working electrode, provides an efficient transport route

Table 1
Photovoltaic performance under illumination conditions of AM1.5G, 1000 W/m² for glass/ITO/PCBM:P3HT/Au structure (device A), glass/ITO/TiO₂(0.005 M)/PCBM:P3HT/Au structure (device B), and glass/ITO/TiO₂ (0.01 M)/PCBM:P3HT/Au structure (device C)

Devices	J_{SC} (mA/cm²)	V_{OC} (mV)	FF (%)	η (%)
A	4.0	105	30	0.13
B	6.0	148	30	0.27
C	8.7	246	40	0.85

J_{SC} is the short-circuit current density, V_{OC} is the open-circuit voltage, FF is the fill factor and η is the conversion efficiency.
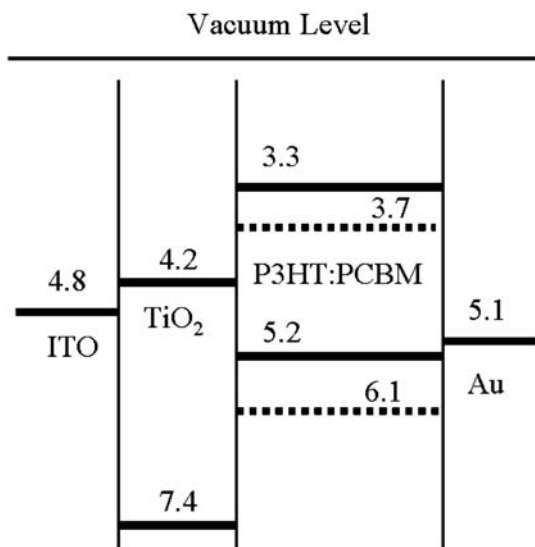
Fig. 5. Energy diagram of ITO/ TiO$_2$/ P3HT:PCBM /Au photovoltaic cells.

for the photo-generated electrons from the excited dye to be injected into the conduction band of the titanium dioxide. In the case of our solar cells, the TiO$_2$ layer between the ITO and active polymer layer not only works as a hole blocking layer but also favors the transport of electrons from the active polymer layer into the collecting electrodes. Fig. 5 shows the energy band diagram of the solar cells. From this diagram, it can be seen that the oxide film modifies the work function of the anode contact from 4.8 eV (ITO) to 4.2 eV (TiO$_2$), which produces a strong driving force resulting from the band offset between the conduction band edge of TiO$_2$ and lowest unoccupied molecular orbital level of PCBM. This electron-withdrawing contact leads to a higher electron transfer from PCBM to TiO$_2$. Thus, the solar cells with an buffer TiO$_2$ layer between ITO and PCBM:P3HT will have a higher short-circuit current density (J_{SC}) than that of similar devices without TiO$_2$. In addition, comparing the fill factor of cells with and without a TiO$_2$ layer, the FF value of those using an oxide film would be higher because of the reduction of total series resistance of devices. We also note that the performance of device C is better than that of device B, which can be explained by the difference in morphology of the oxide film. In fact, the surface of the TiO$_2$ film in device C is granular compared to that of device B, and this morphology may enhance the contact area between the oxide and the polymer films, leading to a better charge injection. However, when the fill factor of the best device is still low (~40%) and may be further improved by optimizing the thickness of the TiO$_2$ layer to minimize the overall series resistance of devices.

The bulk heterojunction cells, which consists of a blending of donor and acceptor materials to create a phase segregated, interpenetrating network provides a large dispersed interface resulting in the efficient exciton dissociation and charge transport within the respective network path. The use of a bulk heterojunction structure has several advantages over a planar heterojunction one. First, the interface area is larger in the former, enhancing the carrier transfer. Second, the distance for the excitons to reach the interface is shorter in these devices providing more available excitons within the diffusion length

and the dissociation of the photo-induced charges is much more efficient. In similar device structure having a planar heterojunction [19], the short-circuit current density is reported to be much lower than those determined in our devices.

4. Conclusion

In summary, we have investigated the deposition process parameters of TiO$_2$ using LPD technique. It was found that ITO substrates are suitable for depositing thin, uniform and smooth oxide films by controlling especially the concentration of the precursor solution. The oxide films have been analysed by several spectroscopic techniques and identified as the anatase phase. The ITO/TiO$_2$ substrates were then used for making photovoltaic cells having a polymer blend as an active layer. The performances of the cells have been determined and compared with those having no TiO$_2$ layer. An improvement of performance is observed and explained by the specific role of the TiO$_2$ in the modification of the contact surface between the oxide and the polymer and also in the change of the work function difference between these films.

References

[1] G.P. Burns, J. Appl. Phys. 65 (1989) 2095.
[2] M.A. Butler, D.C. Ginley, J. Mater. Sci. 15 (1980) 19.
[3] T. Carlson, G.L. Griffin, J. Phys. Chem. 90 (1986) 5896.
[4] S.H. Yang, T.P. Nguyen, P. Le Rendu, C.S. Hsu, Thin Solid Films 471 (2005) 230.
[5] H. Nagayama, H. Honda, H. Kawahara, J. Electrochem. Soc. 135 (1988) 2013.
[6] A. Hishinuma, T. Goda, M. Kitaoka, S. Hayashi, H. Kawahara, Appl. Surf. Sci. 48/49 (1991) 405.
[7] S. Deki, Y. Aoi, O. Hiroi, A. Kajinami, Chem. Lett. 6 (1996) 433.
[8] B. O'Regan, M. Grätzel, Nature 353 (1991) 737.
[9] U. Bach, D. Lupo, P. Comte, J.E. Moser, F. Weissörtel, J. Salbeck, H. Spreitzer, M. Grätzel, Nature 395 (1998) 583.
[10] A.C. Arango, L.R. Johnson, V.N. Blizyuk, Z. Schlesinger, S.A. Carter, H.H. Hörhold, Adv. Mater. 12 (2000) 1689.
[11] A.J. Breeze, Z. Schlesinger, S.A. Carter, P.J. Brock, Phys. Rev. B 64 (2001) 125.
[12] P.A. van Hal, M.M. Winkm, J.M. Kroon, W.J.H. Verhees, L.H. Slooff, W.J.H. van Gennip, P. Johkeijm, R.A.J. Janssen, Adv. Mater. 15 (2003) 118.
[13] H. Hänsel, H. Zettl, G. Kraush, R. Kisselev, M. Thelakat, H.W. Schmidt, Adv. Mater. 15 (2003) 2056.
[14] M. Thelakkat, C. Schmitz, H.W. Schmidt, Adv. Mater. 14 (2002) 577.
[15] D. Huang, Z.D. Xiao, J.H. Gu, N.P. Huang, C.W. Yuan, Thin Solid Films 305 (1997) 110.
[16] K. Kato, K. Niihata, Thin Solid Films 298 (1997) 76.
[17] M. Mossadeq-ur-Rahman, G. Yu, T. Soga, T. Jimbo, H. Ebisu, M. Umeno, J. Appl. Phys. 88 (2000) 4634.
[18] S.E. Shaheen, C.J. Barbec, N.S. Sariciftci, Appl. Phys. Lett. 78 (2001) 841.
[19] Y. Liu, M.A. Summers, C. Edder, J.M.J. Fréchet, M.D. McGehee, Adv. Mater. 17 (2005) 2960.